Talanta 225 (2021) 121963

Contents lists available at ScienceDirect

Talanta

journal homepage: www.elsevier.com/locate/talanta

Silver-amplified fluorescence immunoassay via aggregation-induced emission for detection of disease biomarker

Ze-Hui Sun [a,1], Xuan-Xuan Zhang [a,1], Duo Xu [a], Jie Liu [a], Ru-Jia Yu [a], Chao Jing [a], Huan-Xing Han [b,**], Wei Ma [a,*]

[a] School of Chemistry & Molecular Engineering, East China University of Science and Technology, 130 Meilong Road, Shanghai, 200237, PR China
[b] Translational Medicine Center, Changzheng Hospital, The Second Military Medical University, PR China

ARTICLE INFO

Keywords:
Disease biomarker
Fluorescence immunoassay
Enzyme-free amplification
Aggregation induced emission
Biosensor

ABSTRACT

Development of simple, robust, and reliable detection strategy of disease biomarkers holds tremendous promise for early clinical diagnosis and prognosis of diseases. In this work, through combining a silver nanoparticle (AgNP) linked immunoassay and aggregation induced emission (AIE)-based fluorogenic Ag^+ probe, we developed a silver-amplified fluorescence immunoassay for the detection of disease biomarkers. This method overcame the intrinsic limitations of enzymes as the dissolution of AgNPs generated numerous Ag^+, which could switch on the fluorogenic Ag^+ probe driven by tetrazolate-Ag^+ complexation. As a proof of concept, our method could be used for determining α-fetoprotein (AFP) with a linear relationship in concentrations ranging from 0.1 ng mL^{-1} to 5 μg mL^{-1} and a low limit of detection of 42 pg mL^{-1}. Our method was successfully confirmed for the detection of AFP in real serum samples from hepatocellular carcinoma (HCC) patients, demonstrating the great potential for clinical diagnosis.

1. Introduction

Ultrasensitive detection of disease biomarkers in clinical samples is crucial for early diagnosis and treatment of disease [1–6]. Up to now, enzyme-linked immunosorbent assay (ELISA), which based on specific reactions of antigen-antibody and biocatalytic amplification of enzyme, has been developed as the most commonly used method because of its simplicity, rapidness and high-throughput [7–9]. Enzymes, play a crucial role in the ELISA method for signal amplification, are cost-consuming and are generally sensitive to reaction conditions like pH, temperature and inhibitors, etc [10–13]. Therefore, it is of vital significance to develop new strategy for the ultrasensitive detection of disease biomarkers without enzyme amplification. Recently, the dissolution of metal nanoparticles into ions has been proposed to serve as an alternative approach which exhibits comparable amplification with the enzymes [4,8]. A robust metal-linked immunosorbent assay (MeLISA) with colorimetric readout has been developed for the ultrasensitive detection of cancer biomarkers [1].

With the rapid development of inorganic quantum dots and organic fluorophores, fluorescence has drawn increasing attention in bioanalyte sensing with high sensitivity [14–19]. One of the bottlenecks to perform fluorescence detection is the high background fluorescence of the conventional fluorescent materials and the aggregation-caused quenching effect at high concentration [20–23]. Accordingly, a new type of fluorescence molecules with the unique AIE properties has been developed over the past decade [24–28]. Aggregation-induced emission luminogens (AIEgens) display the negligible or weak emission in solution but exhibit the strong emitting in aggregates or solid state [29]. Comparing with the traditional aggregation-caused quenching luminogens, AIEgens have better photostability and higher brightness, which are highly suitable for high quality fluorescent visualizers for biological imaging and excellent fluorescence tracking for sensing [24,26,30,31]. Considering the AIEgen is convenient and sensitive, the strategy is furthermore plausible for developing a new AIE immunoassay. In previous study, atetrazole-tagged aggregation induced emission (AIE) luminogen, driven by tetrazolate-Ag^+ interactions, was introduced as a novel water-soluble fluorogenic Ag^+ probe [15]. On this basis, we presented a silver-amplified fluorescence immunoassay using this AIE probe for the

* Corresponding author.
** Corresponding author.,
E-mail addresses: huanxing_han@163.com (H.-X. Han), weima@ecust.edu.cn (W. Ma).
[1] These authors contributed equally.

https://doi.org/10.1016/j.talanta.2020.121963
Received 14 August 2020; Received in revised form 24 November 2020; Accepted 1 December 2020
Available online 16 December 2020

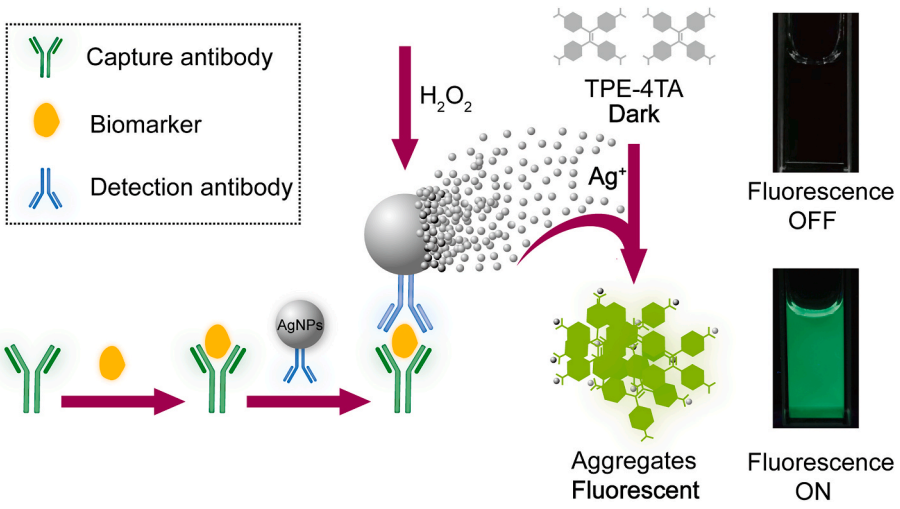

Scheme 1. Schematic diagram of silver-amplified fluorescence immunoassay through the combination of particle-to-ions (AgNP-to-Ag^+) amplification and Ag^+-tetrazolate triggered AIE process for the detection of disease biomarkers.

ultrasensitive detection of disease biomarkers in this study (Scheme 1). Instead of enzymes used in traditional ELISA, AgNPs-labeled detection antibody was utilized as the signal amplification. With the addition of mild H_2O_2 solution, AgNP-Ab could be dissolved into millions of Ag^+, which induced the aggregation of fluorogenic Ag^+ probe. Single AgNP produces a large amount of Ag^+ by several orders of magnitude through the particle-to-ions amplification, and then Ag^+ switches on the fluorescence of AIEgens molecules via an Ag^+-triggered aggregation reaction. Because the amount of target biomarkers in the system was directly related to the number of AgNPs, it was easy to directly detect Ag^+ by fluorescence detection technology and further use it for biomarker detection. Using AFP as a model biomarker, we demonstrated that this fluorescence immunoassay displayed high sensitivity for AFP with detection limit as low as 42 pg mL^{-1}. Our method was successfully confirmed for the detection of AFP in real serum samples from HCC patients. With these merits, we believed our proposed silver-amplified fluorescence immunoassay via aggregation-induced emission was available to rapid detection of other disease biomarkers for clinical applications.

2. Experimental section

2.1. Materials and reagents

All reagents used for all experiments were of analytical grade and were used without further purification. Sodium hydroxide (NaOH, 97%) was obtained from Shanghai Aladdin Reagent Co., Ltd (China). Sodium citrate (Na_3Cit), nitric acid (HNO_3), hydrochloric acid (HCl), disodium hydrogen phosphate ($Na_2HPO_4{\cdot}12H_2O$), sodium dihydrogen phosphate ($NaH_2PO_4{\cdot}2H_2O$) and hydrogen peroxide (H_2O_2, 30%) were purchased from Shanghai Lingfeng Chemical Reagent Co., Ltd. (China). Silver nitrate ($AgNO_3$) was purchased from Sinopharm Chemical Reagent Co., Ltd. (Shanghai, China). Tween-20 was purchased from Acros. Bovine serum albumin (BSA, ≥98.0%) was purchased from Sigma-Aldrich. 96-well polystyrene plates were purchased from Corning Incorporated. The tetrazole-tagged AIE luminogen (TPE-4TA) was obtained from AIEgen Biotech Co. Ltd. Human AFP ELISA kits were obtained from Shanghai MLBIO Biotechnology Co. Ltd. Ultrapure water with a resistivity of 18.2 MΩ cm produced by a Millipore system was used throughout the experiment. A real sample of clinical diagnosis of AFP antigens, antibodies, prostate specific antigen (PSA), procalcitonin (PCT), hepatitis B virus surface antigen (HBsAg) were provided by the Prof. H.X.H.

2.2. Apparatus

Fluorescence spectra were obtained with a Synergy H4 Hybrid Reader (BioTek Instrument, Inc., America). Transmission electron microscopy (TEM) images were collected with a JEOL 2100 electron microscope (JEOL Ltd., Japan). Ultraviolet–visible absorption spectra were acquired with an Ocean Optics instrument.

2.3. Synthesis of 60 nm AgNPs

The AgNPs with an average diameter of 60 nm were synthesized via the following steps [32,33]. Briefly, 18 mg $AgNO_3$ was dissolved in 100 mL of ultrapure water and heated to boiling. Then a 2 mL of sodium citrate solution (1%) was added in the boiling solution and kept on boiling for 15 min. The AgNPs solutions were stored in dark bottles after cooling to room temperature.

2.4. Conjugation of AgNPs to detection antibody

AgNPs-labeled detection antibody was prepared by electrostatic adhesion method. Typically, 1 mL of as-prepared AgNPs was condensed by centrifugation and then redispersed in 1 mM PBS of pH 7.4 (avoiding chloridion), to which 50 μL of diluted detection antibody (diluted 250 times with 1 mM PBS, 1.2×10^{-7} M) was added. The mixture was shaken for 12 h and then blocked for 12 h with 1% BSA. Then, the solution was repeatedly centrifuged under optimized conditions to get rid of the excess antibody. AgNPs-Ab (AgNPs conjugated with detection antibody) was dispersed in 0.1% BSA. Finally, the resulting AgNPs-Ab solution was stored at 4 °C before use.

2.5. Sandwich assay for AFP

Firstly, 100 μL of the capture antibody diluted 2000 times in PBS (20 mM, pH 7.4) was immobilized on the 96-well polystyrene plates at 4 °C overnight. After removing the excess captured antibodies, the polystyrene plate was washed five times using 350 μL of PBST solution. Blocking buffer (200 μL of 1% BSA) was further added and incubated at room temperature for 2 h. And then washing five times with PBST solution, 100 μL of AFP at different concentrations from 10^{-12} g mL^{-1} to 5×10^{-6} g mL^{-1} were added to the plates, and the blank was set as negative control by adding buffer only, then the plate was incubated at 37 °C for 1 h. Washing steps were performed again and subsequently 100 μL of AgNPs-Ab dissolved in blocking buffer was added at 37 °C for 1 h. Followed by five times washing to remove naked AgNPs and

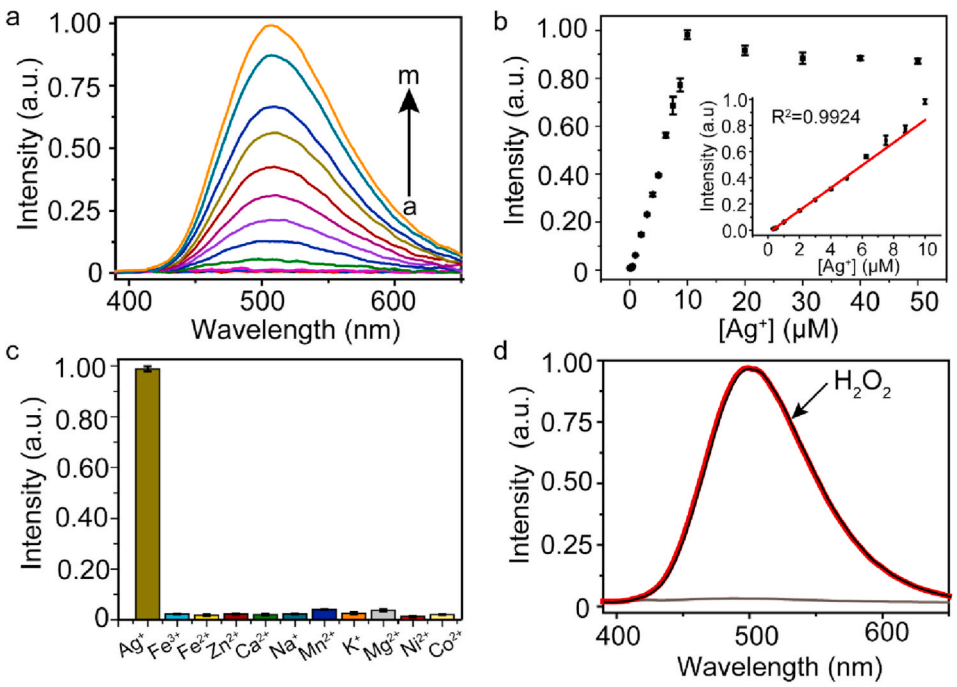

Fig. 1. Characterization of Ag^+-induced fluorogenic aggregation system. (a) Fluorescence response of 10 μM TPE-4TA at different concentrations of Ag^+ from a to m: 0, 0.3, 0.4, 0.5, 1.0, 2.0, 3.0, 4.0, 5.0, 6.25, 7.5, 8.75 and 10 μM (ex: 368 nm; em: 500 nm); (b) Plot of fluorescence intensity of 10 μM TPE-4TA at 504 nm as a function of the concentrations of Ag^+; inset: The linear plots of the fluorescence intensity of TPE-4TA as function of the concentrations of Ag^+. (c) Fluorescence histogram of different metal ions on the molecular response of the probe (including Ag^+, Fe^{3+}, Fe^{2+}, Zn^{2+}, Ca^{2+}, Na^+, Mn^{2+}, K^+, Mg^{2+}, Ni^{2+} and Co^{2+}). The concentration of metal ions was 5 μM and the probe concentration was 10 μM. (d) Fluorescence intensity of TPE-4TA in water (gray line), TPE-4TA in the presence of 5 μM Ag^+ with (black line) and without 5 mM H_2O_2 (red line), respectively. (For interpretation of the references to color in this figure legend, the reader is referred to the Web version of this article.)

residual AgNPs-Ab, the prepared 96-well polystyrene plate was placed in a refrigerator at 4 °C for the next use. Error bar represents the standard deviations of measurements from three independent experiments.

2.6. Fluorescent detection for biomarker protein

The amplification effect of this experiment was achieved by dissolving AgNPs in the presence of H_2O_2 to produce millions of Ag^+. In detail, 50 μL of H_2O_2 (5 mM) was added into each well, and reacted at room temperature for 10 min to fully dissolve the 60 nm AgNPs into Ag^+. Next, the solution in each well was reacted with 50 μL of TPE-4TA (10 μM). The fluorescence intensity of each well was further measured by Synergy H4 Hybrid Reader.

2.7. Assays of clinical serum samples

To confirm the feasibility of the detection strategy for clinical samples, a total of 19 clinical serum samples were collected from patients

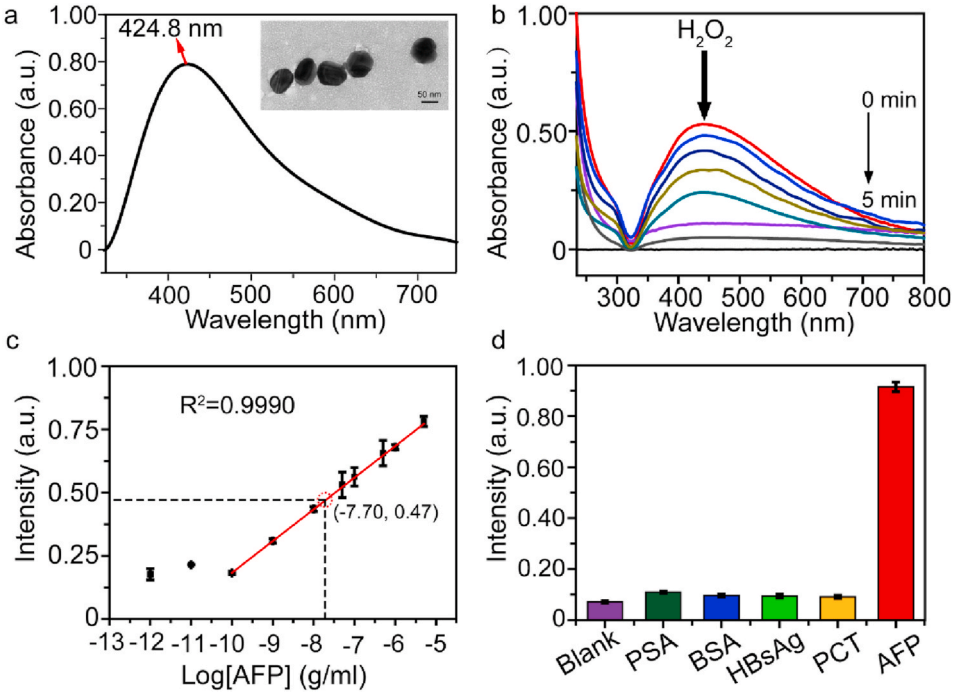

Fig. 2. Silver-amplified fluorescence immunoassay for AFP detection. (a) UV–vis spectrum and typical TEM image (inset) of the as-prepared AgNPs. (b) UV–Vis spectra of AgNPs solution with the dissolution time in the presence of 5 mM H_2O_2. (c) Plot of the fluorescence intensity as function of the concentrations of AFP from 10^{-12} to 5×10^{-6} g mL^{-1}. The error bar represents the standard deviation from three independent measurements. (d) Detection specificity of our method.

Table 1
Performance comparison of the current work with other reported fluorescence immunoassays for the detection of AFP.

Fluorogenic probe		LOD (pg mL^{-1})	Dynamic range (ng mL^{-1})	Ref.
Inorganic nanomaterials	FRET of a sandwich structured QDs-AFP-AuNPs	400	0.5 to 45	37
	Nano graphite carbon nitride	430	5 to 600	38
Organic dye molecules	Rhodamine-based fluorogenic probe	70	0.1 to10	20
	Polyfluorene-based cationic conjugated polyelectrolytes	176	0 to 1000	39
	Metal coordination polymer induced perylene excimer fluorescence	400	0 to 20	40
	Aggregation-induced emission fluorogenic probe	42	0.1 to 5000	this work

with hepatocellular carcinoma and normal subjects, regarding as positive and negative samples, respectively. All serum samples were stored at −80 °C until use. The subsequent detection procedures were identical to sandwich assay for AFP detection just by replacing the AFP standards with diluted 10 times sera, and the results were obtained in Synergy H4 Hybrid Reader for convenience.

3. Results and discussion

3.1. Fluorescence response of fluorogenic Ag^+ probe (TPE-4TA) in the presence of Ag^+

Inspired by the fact that 1/2*H*-tetrazole compounds have been well-known to efficiently precipitate out Ag^+ from a solution, a tetrazole-tagged AIE luminogen (TPE-4TA) as the fluorogenic Ag^+ probe can be rationally achieved via an Ag^+-triggered aggregation reaction [15,34]. Before the following immunoassay experiments for the detection of disease biomarkers, the fluorescence response of TPE-4TA to Ag^+ at different concentrations was investigated in priority under 368 nm excitation. As shown in Fig. 1a, the fluorescence intensity of TPE-4TA gradually increased upon addition of increasing concentrations of Ag^+ at the maximum intensity of 504 nm, with a good linearity with R^2 = 0.9924 in the range of Ag^+ from 300 nM to 10 μM. With a further addition of Ag^+ concentration to 10 μM, fluorescence saturation was reached approximately (Fig. 1b). Like a typical AIE molecule, TPE-4TA has a flexible structure in solution and emits faintly because of the free rotational motion of the phenyl rings. After the addition of Ag^+ to TPE-4TA, silver atom can bind with the N atoms of the tetrazole ring to trigger aggregation through infinite metal-coordination complexation [15,35]. Therefore, an instantaneous fluorescence was observed for nano-sized tetrazole silver aggregates due to the aggregation-induced fluorescence effect.

To further confirm the specificity of the TPE-4TA to Ag^+, we also evaluated the fluorescence response of TPE-4TA with interfering H_2O_2 and different kind of metal ions, including Ag^+, Fe^{3+}, Fe^{2+}, Zn^{2+}, Ca^{2+}, Na^+, Mn^{2+}, K^+, Mg^{2+}, Ni^{2+} and Co^{2+}. These results showed that negligible change in fluorescence intensities was observed for these interfering metal ions (Fig. 1c). Considering the dissolution process of AgNPs, we also investigated the interference effect of H_2O_2 to fluorescence detection system of TPE-4TA. Notably, TPE-4TA did not exhibit fluorescence quenching in 5 mM of H_2O_2 solution, indicating that this fluorogenic Ag^+ probe could not be influenced by the dissolution process of AgNPs (Fig. 1d). This is because that H_2O_2 does not have a coordination structure with the nitrogen at the tetrazole moiety, resulting in a negligible contribution to TPE-4TA aggregation [34]. Taken together, the Ag^+-tetrazolate aggregation-triggered AIEgen of TPE-4TA can be used in fluorescence immunoassay due to the high stability and high selectivity to produce a robust fluorescence signal. However, our detection method is not suitable for the immunoassay system of existed Hg^{2+} because Hg^{2+} may have similar response due to the similar mercury-tetratezolate coordination (data not shown) [15,36].

3.2. Fluorescence detection of disease biomarkers using the silver-amplified fluorescence immunoassay

Inspired by the sensitivity and selectivity of Ag^+-triggered fluorescence detection system, we attempted to determine the disease biomarkers through combining a AgNP-linked immunoassay and Ag^+-triggered AIEgen probe. Firstly, 60 nm of AgNPs (Fig. 2a) and the polystyrene plate were biofunctionalized with detection antibodies and capture antibodies, respectively, using an optimal procedure that ensures the ultralow fouling capability and the strong recognition efficiency. This silver-amplified fluorescence immunoassay involves two important steps to amplify the signal response and to enhance the recognition selectivity. First, the AgNPs-labeled detection antibodies (AgNP-Ab) were immersed in 200 μL of the sample solution at 37 °C for 1 h to allow recognition of the target biomarkers, AFP, which had been previously conjugated with the capture antibodies immobilized on the surface of polystyrene plate. Second, after dissolving AgNPs, Ag^+ could activate the fluorescence switch-on of TPE-4TA. After the addition of 5 mM H_2O_2 at room temperature, the absorption intensity of AgNPs at 420 nm gradually decreased and finally disappeared within 5 min, indicating the excellent dissolution ability of H_2O_2 (Fig. 2b). Thus, to fully dissolving AgNPs into Ag^+, 10 min incubation by H_2O_2 was used for the dissolution process in this work. Because AgNPs directly associated with the target biomarkers through the sandwich immunoreaction, the concentration of target biomarkers can be conveniently determined by monitoring the variation of the fluorescence intensity of TPE-4TA solution with high sensitivity. Fig. 2c showed a good linear response with the logarithm (lg) of the AFP concentration for a wide range from 0.1 ng mL^{-1} to 5 μg mL^{-1}. The corresponding calibration equation was I_{504} (au) = 1007.50lg (C_{AFP}/g mL^{-1}) + 11539.89 (R^2 = 0.9990, with a detection limit of 42 pg mL^{-1} for AFP, on the basis of 3 N/S). As shown in the compared results with the previously reported fluorescence detection methods (Table 1) [20,37–40] and the conventional ELISA method (Fig. S1) for AFP detection, our method achieved a higher sensitivity and a wider linear range. The point at (−7.70, 0.47) represents the fluorescence intensity value at the clinical threshold of 20 ng mL^{-1}. Because the C_{AFP} in healthy human serum was below 20 ng mL^{-1}, our method was sensitive enough to distinguish the HCC patients and healthy people.

To discriminate bio-recognition signals from non-specific interaction, we further performed a control experiment that comprised replacing the target antigen by the common interferential proteins not specific to capture antibody and detection antibody, including prostate specific antigen (PSA), bovine serum albumin (BSA), familiar pathogen hepatitis B virus surface antigen (HBsAg) and procalcitonin (PCT). In this control experiment, 0.1 μg mL^{-1} of AFP was selected as the concentration of target antigen, and other interferential proteins with a higher concentration of 10 μg mL^{-1} have been used due to the complexities and uncertainties of real serum samples. Notably, the dramatic fluorescence signal was only responded for AFP and the negligible signal change was observed for the other interfering proteins, demonstrating high specificity of this system for the detection of disease biomarker (Fig. 2d).

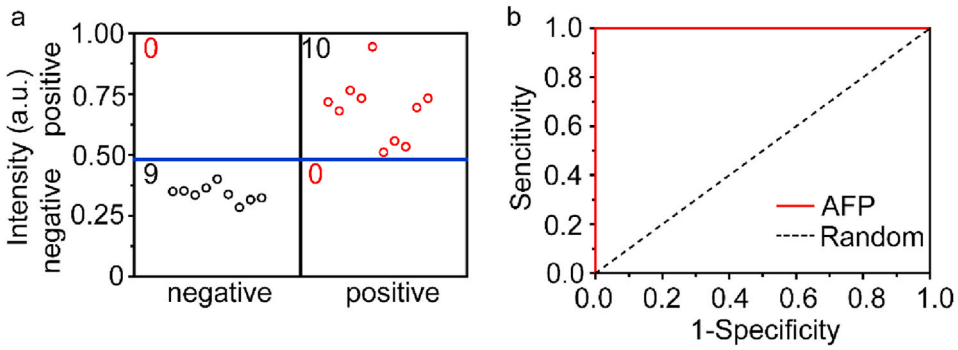

Fig. 3. Fluorescence detection of AFP in real serum samples with double-blind experiment. (a) Vertical scatter plots of the fluorescence intensity for positive serum samples and negative ones. (b) ROC curve describing the sensitivity and specificity for AFP in clinical serum samples.

3.3. Real sample detection by the silver-amplified fluorescence immunoassay

Encouraged by the sensitivity and specificity of silver-amplified fluorescence immunoassay, we further evaluated our method for clinical serum samples. A double-blind measurement was carried out using 19 unrelated clinical serum samples with a 10-fold dilution. Fig. 3a showed that this enzyme-free amplified fluorescence immunoassay could successfully detect AFP and had a good agreement with the clinical results by chemiluminescence immunoassay. Positive and negative serum samples can be differentiated on the basis of cut off values of fluorescence intensity at 504 nm with a clinical threshold of 20 ng mL^{-1}. The blue line was made as a threshold for positive result from HCC patients and negative results from healthy people of our method. 10 AFP positive serum samples and 9 negative ones were effectively differentiated according to the fluorescence response of the resulting solution (Fig. 3a), demonstrating that sensitivity and selectivity of our method were both 100% for AFP. Additionally, the calculated area of the receiver operating characteristic (ROC) curve was 1.0, demonstrating excellent discrimination of the proposed method (Fig. 3b). All results suggested that this silver-amplified fluorescence immunoassay had the potential to facilitate the detection of early-cancer through clinical serum sample tests.

4. Conclusions

In summary, we have developed a simple and robust silver-amplified fluorescence immunoassay for the detection of disease biomarker. In this work, AgNPs was functionalized with the detection antibodies and served as an Ag^+ source bridging the fluorescence response of TPE-4TA and the concentration of disease biomarkers. On the one hand, highly efficient enzyme-free signal amplification can be achieved by the chemical dissolution of AgNPs into Ag^+. On the other hand, Ag^+ would light up the fluorescence signal of the AIE-active probe TPE-4TA with a high signal to noise ratio due to the spontaneous aggregation via the coordination of anionic tetrazolate groups with Ag^+. Using AFP as a disease biomarker, this fluorescence immunoassay method showed high sensitivity for the detection of AFP as low as 42 pg mL^{-1} on the basis of 3N/S. Moreover, an outstanding performance was further confirmed for the clinical diagnosis of HCC patients. We believed that the proposed method has great potential for extension to other disease biomarker for further applications.

CRediT authorship contribution statement

Ze-Hui Sun, Methodology, Investigation, Visualization, Writing – original draft preparation. Xuan-Xuan Zhang, Investigation, Methodology, Visualization, Writing – original draft preparation. Duo Xu, Investigation, Writing – original draft preparation. Jie Liu, Methodology, Investigation. Ru-Jia Yu, Discussion. Chao Jing, Discussion. Huan-Xing Han, Discussion, Resources. Wei Ma, Conceptualization, Methodology, Resources, Supervision, Project administration, Funding acquisition, Writing – original draft preparation, Writing-Reviewing and Editing.

Declaration of competing interest

The authors declare that they have no known competing financial interests or personal relationships that could have appeared to influence the work reported in this paper.

Acknowledgements

This research was supported by Shanghai Pujiang Program (2019PJD010), National Natural Science Foundation of China (21775043), Shanghai Municipal Natural Science Fund (19ZR1472100), Xiamen University Opening Project of PCOSS (201901), Fundamental Research Funds for the Central Universities (JKJ012016013), Shanghai Sailing Program (18YF1405700) and Shanghai Strategic Emerging Industry Major Project (AI/RD2017-03).

Appendix A. Supplementary data

Supplementary data to this article can be found online at https://doi.org/10.1016/j.talanta.2020.121963.

References

[1] R.J. Yu, W. Ma, X.Y. Liu, H.Y. Jin, H.X. Han, H.Y. Wan, , the Fundamental Research Funds for the Central Universities, G.H. Tian, Y.T. Long, Metal-linked immunosorbent assay (MeLISA): the enzyme-free alternative to ELISA for biomarker detection in serum, Theranostics 6 (2016) 1732–1739, 10.7150/thno.16129.

[2] R. Etzioni, N. Urban, S. Ramsey, M. McIntosh, S. Schwartz, B. Reid, J. Radich, G. Anderson, L. Hartwell, The case for early detection, Nat. Rev. Canc. 3 (2003) 243–252, 10.1038/nrc1041.

[3] J.M. Winter, C.J. Yeo, J.R. Brody, Diagnostic, prognostic, and predictive biomarkers in pancreatic cancer, J. Surg. Oncol. 107 (2013) 15–22, 10.1002/jso.23192.

[4] D. Xu, Z.H. Sun, X. Hua, H.X. Han, W. Ma, Y.T. Long, Plasmon-induced photoreduction system Allows ultrasensitive detection of disease biomarkers by silver-mediated immunoassay, ACS Sens. 5 (2020) 2184–2190, 10.1021/acssensors.0c00799.

[5] M.P. Peng, W. Ma, Y.T. Long, Alcohol dehydrogenase-catalyzed gold nanoparticle seed-mediated growth allows reliable detection of disease biomarkers with the naked eye, Anal. Chem. 87 (2015) 5891–5896, 10.1021/acs.analchem.5b00287.

[6] L.X. Cheng, Z.K. Zhang, D. Zuo, W.F. Zhu, J. Zhang, Q.D. Zeng, D.Y. Yang, M. Li, Y. L. Zhao, Ultrasensitive detection of serum MicroRNA using branched DNA-based SERS platform combining simultaneous detection of alpha-fetoprotein for early diagnosis of liver cancer, ACS Appl. Mater. Interfaces 10 (2018) 34869–34877, 10.1021/acsami.8b10252.

[7] J. Satija, N. Punjabi, D. Mishra, S. Mukherji, Plasmonic-ELISA: expanding horizons, RSC Adv. 6 (2016) 85440–85456, 10.1039/C6RA16750K.

[8] X.X. Zhang, D. Xu, D. Guo, H.X. Han, D.W. Li, W. Ma, Enzyme-free amplified SERS immunoassay for the ultrasensitive detection of disease biomarkers†, Chem. Commun. 56 (2020) 2933–2936, 10.1039/C9CC09379F.

[9] R.M. Lequin, Enzyme immunoassay (EIA)/enzyme-linked immunosorbent assay (ELISA), Clin. Chem. 51 (2005) 2415–2418, 10.1373/clinchem.2005.051532.
[10] L.L. Tian, Y. Weizmann, Real-time detection of telomerase activity using the exponential isothermal amplification of telomere repeat assay, J. Am. Chem. Soc. 135 (2013) 1661–1664, 10.1021/ja309198j.
[11] R. Shandilya, A. Bhargava, N. Bunkar, R. Tiwari, I.Y. Goryacheva, P.K. Mishra, Nanobiosensors: point-of-care approaches for cancer diagnostics, Biosens. Bioelectron. 130 (2019) 147–165, 10.1016/j.bios.2019.01.034.
[12] M. Hong, L.D. Xu, Q.W. Xue, L. Li, B. Tang, Fluorescence imaging of intracellular telomerase activity using enzyme-free signal amplification, Anal. Chem. 88 (2016) 12177–12182, 10.1021/acs.analchem.6b03108.
[13] H.H. Ye, K.K. Yang, J. Tao, Y.J. Liu, Q. Zhang, S. Habibi, Z.H. Nie, X.H. Xia, An enzyme-free signal amplification technique for ultrasensitive colorimetric assay of disease biomarkers, ACS Nano 11 (2017) 2052–2059, 10.1021/acsnano.6b08232.
[14] D.S. Chen, X.B. Zhang, L.P. Zhu, C.H. Liu, Z.P. Li, Single microbead-anchored fluorescent immunoassay (smfia): a facile and versatile platform allowing simultaneous detection of multiple antigens, Chem. Asian J. 12 (2017) 2894–2898, 10.1002/asia.201701245.
[15] S. Xie, A.Y.H. Wong, R.T.K. Kwok, Y. Li, H. Su, J.W.Y. Lam, S.J. Chen, B.Z. Tang, Fluorogenic Ag(+) -tetrazolate aggregation enables efficient fluorescent biological silver staining, Angew. Chem. Int. Ed. 57 (2018) 5750–5753, 10.1002/anie.201801653.
[16] C.Y. Zhan, J.T. Cheng, B.W. Li, S.L. Huang, F. Zeng, S.Z. Wu, A fluorescent probe for early detection of melanoma and its metastasis by specifically imaging tyrosinase activity in a mouse model, Anal. Chem. 90 (2018) 8807–8815, 10.1021/acs.analchem.8b00594.
[17] L. Chen, J.W. Lin, J.Q. Yi, Q.H. Weng, Y. Zhou, Z.Z. Han, C.Y. Li, J.H. Chen, Q. Zhang, A tyrosinase-induced fluorescence immunoassay for detection of tau protein using dopamine-functionalized $CuInS_2$/ZnS quantum dots, Anal. Bioanal. Chem. 411 (2019) 5277–5285, 10.1007/s00216-019-01909-9.
[18] A.M. Wagner, J.M. Knipe, G. Orive, N.A. Peppas, Quantum dots in biomedical applications, Acta Biomater. 94 (2019) 46–63, 10.1016/j.actbio.2019.05.022.
[19] J.M. Wang, J. Qian, Z.D. Teng, T. Cao, D.Y. Gong, W. Liu, Y.P. Cao, W.W. Qin, H. C. Guo, A. Iqbal, Self-assembling ratiometric fluorescent micelle nanoprobe for tyrosinase detection in living cells, ACS Appl. Nano. Mater. 2 (2019) 3819–3827, 10.1021/acsanm.9b00689.
[20] L.J. Zhao, R.J. Yu, W. Ma, H.X. Han, H. Tian, R.C. Qian, Y.T. Long, Sensitive detection of protein biomarkers using silver nanoparticles enhanced immunofluorescence assay, Theranostics 7 (2017) 876–883, 10.7150/thno.17575.
[21] Y.F. Zhao, C. Chang, P.P. Gai, L. Han, F. Li, B. Li, One-step synthesis of fluorescent organic nanoparticles: the application to label-free ratiometric fluorescent pH sensor, Sensor. Actuator. B Chem. 273 (2018) 1479–1486, 10.1016/j.snb.2018.07.047.
[22] Z.K. Wang, S.J. Chen, J.W. Lam, W. Qin, R.T. Kwok, N. Xie, Q.L. Hu, B.Z. Tang, Long-term fluorescent cellular tracing by the aggregates of AIE bioconjugates, J. Am. Chem. Soc. 135 (2013) 8238–8245, 10.1021/ja312581r.
[23] W.H. Zhang, W. Ma, Y.T. Long, Redox-mediated indirect fluorescence immunoassay for the detection of disease biomarkers using dopamine-functionalized quantum dots, Anal. Chem. 88 (2016) 5131–5136, 10.1021/acs.analchem.6b00048.
[24] D.D. La, S.V. Bhosale, L.A. Jones, S.V. Bhosale, Tetraphenylethylene-based AIE-active probes for sensing applications, ACS Appl. Mater. Interfaces 10 (2018) 12189–12216, 10.1021/acsami.7b12320.
[25] S.S. Liow, Q.Q. Dou, D. Kai, Z.B. Li, S. Sugiarto, C.Y. Yu, R.T. Kwok, X. Chen, Y. L. Wu, S.T. Ong, A. Kizhakeyil, N.K. Verma, B.Z. Tang, X.J. Loh, Long-Term real-time in vivo drug release monitoring with AIE thermogelling polymer, Small 13 (2017) 1603404, 10.1002/smll.201603404.
[26] R. Hu, A.J. Qin, B.Z. Tang, AIE polymers: synthesis and applications, Prog. Polym. Sci. 100 (2020) 101176, 10.1016/j.progpolymsci.2019.101176.
[27] R.R. Hu, Y. Kang, B.Z. Tang, Recent advances in AIE polymers, Polym. J. 48 (2016) 359–370, 10.1038/pj.2016.1.
[28] G.X. Feng, B. Liu, Aggregation-induced emission (AIE) dots: emerging theranostic nanolights, Acc. Chem. Res. 51 (2018) 1404–1414, 10.1021/acs.accounts.8b00060.
[29] X.X. Gu, R.T.K. Kwok, J.W.Y. Lam, B.Z. Tang, AIEgens for biological process monitoring and disease theranostics, Biomaterials 146 (2017) 115–135, 10.1016/j.biomaterials.2017.09.004.
[30] Y.H. Li, W.G. Wang, Z.Y. Zhuang, Z.M. Wang, G.W. Lin, P.C. Shen, S.M. Chen, Z. J. Zhao, B.Z. Tang, Efficient red AIEgens based on tetraphenylethene: synthesis, structure, photoluminescence and electroluminescence, J. Mater. Chem. C 6 (2018) 5900–5907, 10.1039/C8TC01612G.
[31] L.Z. Li, M. Chen, H.K. Zhang, H. Nie, J.Z. Sun, A.J. Qin, B.Z. Tang, Influence of the number and substitution position of phenyl groups on the aggregation-enhanced emission of benzene-cored luminogens, Chem. Commun. 51 (2015) 4830–4833, 10.1039/C5CC00241A.
[32] Y.W. Zhang, S. Liu, L. Wang, X.Y. Qin, J.Q. Tian, W.B. Lu, G.H. Chang, X.P. Sun, One-pot green synthesis of Ag nanoparticles-graphene nanocomposites and their applications in SERS, H_2O_2, and glucose sensing, RSC Adv. 2 (2012) 538–545, 10.1039/c1ra00641j.
[33] J. Huang, G.W. Zhan, B.Y. Zheng, D.H. Sun, F.F. Lu, Y. Lin, H.M. Chen, Z.D. Zheng, Y.M. Zheng, Q.B. Li, Biogenic silver nanoparticles by cacumen platycladi extract: synthesis, formation mechanism, and antibacterial activity, Ind. Eng. Chem. Res. 50 (2011) 9095–9106, 10.1021/ie200858y.
[34] J.H. Lee, S. Kang, J.Y. Lee, J.H. Jung, A tetrazole-based metallogel induced with Ag^+ ion and its silver nanoparticle in catalysis, Soft Matter 8 (2012) 6557–6563, 10.1039/C2SM25316J.
[35] R. Jason Herr, 5-Substituted-1H-tetrazoles as carboxylic acid isosteres: medicinal chemistry and synthetic methods, Bioorg. Med. Chem. 10 (2002) 3379–3393, 10.1016/S0968-0896(02)00239-0.
[36] S. Chen, W.J. Wang, M.M. Yan, Q. Tu, S.W. Chen, T.B. Li, M.S. Yuan, J.Y. Wang, 2-Hydroxy benzothiazole modified rhodol: aggregation-induced emission and dual-channel fluorescence sensing of Hg^{2+} and Ag^+ ions, Sensor. Actuator. B Chem. 255 (2018) 2086–2094, 10.1016/j.snb.2017.09.008.
[37] L. Zhou, F.H. Ji, T. Zhang, F. Wang, Y.C. Li, Z.X. Yu, X.P. Jin, B. Ruan, An fluorescent aptasensor for sensitive detection of tumor marker based on the FRET of a sandwich structured QDs-AFP-AuNPs, Talanta 197 (2019) 444–450, 10.1016/j.talanta.2019.01.012.
[38] Y.K. Li, L.Y. Dong, X.F. Wang, Y. Liu, H.L. Liu, M.X. Xie, Development of graphite carbon nitride based fluorescent immune sensor for detection of alpha fetoprotein, Spectrochim. Acta Mol. Biomol. Spectrosc. 196 (2018) 103–109, 10.1016/j.saa.2018.02.012.
[39] B.Q. Bao, P. Su, J. Zhu, J. Chen, Y. Xu, B.B. Gu, Y.F. Liu, L.H. Wang, Rapid aptasensor capable of simply detect tumor markers based on conjugated polyelectrolytes, Talanta 190 (2018) 204–209, 10.1016/j.talanta.2018.07.072.
[40] Y.X. Li, S.H. Yin, J.Z. Hou, L.J. Meng, M.J. Gao, Y.C. Sun, C.Z. Zhang, S. Bai, J. Ren, C. Yu, Metal coordination polymer induced perylene probe excimer fluorescence and its application in acetylcholinesterase sensing and alpha-fetoprotein immunoassay, Analyst 144 (2019) 2034–2041, 10.1039/C8AN02231C.